1 A UNIQUE PREDATOR IN A UNIQUE ECOSYSTEM: MODELLING THE APEX

2 PREDATOR FROM THE LATE CRETACEOUS CROCODYLIFORM-DOMINATED

3 FAUNA IN BRAZIL

4

5

6 FELIPE C. MONTEFELTRO[1], STEPHAN LAUTENSCHLAGER[2], PEDRO L. GODOY[3],

7 GABRIEL S. FERREIRA[4], RICHARD J. BUTLER[2]

8 [1]Laboratório de Paleontologia e Evolução de Ilha Solteira, UNESP, Ilha Solteira, Brazil.

9 [2]School of Geography, Earth and Environmental Sciences, University of Birmingham,

10 Birmingham, UK.

11 [3]Department of Anatomical Sciences, Stony Brook University, Stony Brook, USA

12 [4]Departamento de Biologia, Faculdade de Filosofia, Ciências e Letras de Ribeirão Preto,

13 Universidade de São Paulo, Ribeirão Preto, Brazil.

14 *felipecmontefeltro@gmail.com*, *s.lautenschlager@bham.ac.uk*, *pedrolorenagodoy@gmail.com*,

15 *gsferreirabio@gmail.com*, *r.butler.1@bham.ac.uk*

16
17

18   ABSTRACT

19   Theropod dinosaurs were relatively scarce in the Late Cretaceous ecosystems of

20   southeast Brazil. Instead, the abundant hypercarnivore crocodyliforms known as

21   baurusuchids were probably playing the ecological role as apex predators. Baurusuchids

22   exhibited a series of morphological adaptations associated to this ecological role, but

23   quantitative biomechanical assessments to support this were lacking to date. Here, we

24   employ a biomechanical modelling approach, using finite element analysis (FEA) on

25   skull and mandible models of a baurusuchid specimen, allowing us to characterise the

26   craniomandibular apparatus of baurusuchids, as well as to test the hypothesis that their

27   functional morphology allowed them to outcompete other carnivores, such as theropods.

28   Our results demonstrate, for the first time, the ecological role of this group as

29   specialised apex predators in the continental Late Cretaceous ecosystems of South

30   America. With a with a relatively weak bite force (~600 N), baurusuchids preying

31   strategies probably relied on other morphological specializations, such as ziphodont

32   dentition and strong cervical musculature. Consistently, comparative assessments of the

33   stress distribution and magnitude of scaled models of other predators (the theropod

34   *Allosaurus fragilis* and the living crocodylian *Alligator mississippiensis*) show

35   discrepant responses to loadings under the same functional scenarios, further suggesting

36   considerably distinct predatory behaviors for these animals. The unique selective

37   pressures from the arid to semi-arid Late Cretaceous palaeoecosystems of southeast

38   Brazil, which were dominated by crocodyliforms, possibly drove the emergence and

39   evolution of such exclusive set of biomechanical features seen in baurusuchids, which

40   had not been previously reported for any other predatory taxon.

41

42

43   INTRODUCTION

44   In nearly all known continental Cretaceous ecosystems worldwide, the dominant

45   hypercarnivores and apex predators were theropod dinosaurs (Lloyd *et al*. 2008; Benson

46   *et al*. 2013; Zanno & Mackovicky 2013). However, in the Late Cretaceous ecosystems

47   of Brazil, theropods were exceptionally scarce. Instead, the putative dominant apex

48   predators were a group of large, terrestrial crocodyliforms, the baurusuchids (Riff &

49   Kellner 2011; Godoy *et al*. 2014). Baurusuchids are phylogenetically included within

50   Notosuchia, a group of highly diverse crocodyliforms which thrived mainly in

51   Gondwana during the Cretaceous (Pol & Leardi 2015; Mannion *et al*. 2015). Exhibiting

52   a wide range of morphological variation, from gracile omnivores to pug-nosed

53   herbivores, notosuchians contributed significantly to the highest peak of morphological

54   disparity experienced by crocodyliforms (Wilberg 2017; Godoy 2019; Godoy *et al*.

55   2019).

56   Although present in other parts of Gondwana, most baurusuchids species (ca.

57   80%) are found in the Late Cretaceous rocks of the Bauru Group, in southeast Brazil

58   (Carvalho *et al*. 2005; Godoy *et al*. 2014; Montefeltro *et al*. 2011). The Bauru Group

59   palaeoecosystem witnessed an extraordinary abundance of notosuchians, with nearly 30

60   species described so far. Dinosaurs were also present, but their fossil record is relatively

61   poorer for these rocks. Within this crocodyliform-dominated ecosystem, baurusuchids

62   formed the likely apex predators. Baurusuchids exhibited a series of morphological

63   adaptations associated with their role as hypercarnivores, possibly achieved via

64   heterochronic transformations, such as hypertrophied canines, a reduced number of

65   teeth, and dorsoventrally high skulls (Montefeltro *et al*. 2011; Riff & Kellner 2011;

66   Godoy *et al*. 2018). Yet, quantitative assessments about the paleobiology of

67   baurusuchids are lacking, and the data supporting the apex-predatory role of the

68   baurusuchids is primarily derived from broad generalizations and the faunal

69   composition of the Bauru ecosystem (Riff & Kellner 2011; Godoy *et al.* 2014).

70   Here, we employ a biomechanical modelling approach to test the hypothesis that

71   the cranial functional morphology allowed baurusuchids to outcompete other

72   archosaurian carnivores. Using finite element analysis (FEA) we characterize the

73   baurusuchid skull biomechanically and quantify functional similarities and differences

74   between baurusuchids, theropod dinosaurs and living crocodylians. We also calculate

75   bite forces and simulate different functional scenarios to reveal biomechanical

76   properties of the baurusuchid skull and to understand how this group dominated the

77   unique crocodyliform-dominated ecosystems during Cretaceous in Brazil.

78

79   MATERIALS AND METHODS

80   **Specimens.** The baurusuchid specimen modelled for the present study is a complete

81   skull with lower jaws, referred to *Baurusuchus pachecoi* (LPRP/USP 0697 Laboratório

82   de Paleontologia USP-RP) and collected in Jales, Brazil (Adamantina Formation, Bauru

83   Group; Montefeltro 2019). For comparisons, we also modelled a specimen of the

84   theropod *Allosaurus fragilis* (MOR 693, Museum of the Rockies, Bozeman) and one

85   specimen of *Alligator mississippiensis* (XXXXXXXX). *Allosaurus fragilis* was chosen

86   based on its medium size when compared to other theropods, which is equivalent to the

87   putative size of the theropods from the Adamantina Formation, for which no complete

88   craniomandibular material is known. *Allosaurus* has been proposed to be functionally

89   similar to abelisaurids, the most commonly found theropods in the Bauru Group

90   (Sakamoto 2010). Furthermore, the choice of *Alligator mississippiensis* for the

91   comparison with a living representative of the crocodyliform lineage was also made

92   given that this is a model organism for herpetological and functional studies (Guillette

93   *et al*. 2007; Farmer & Sanders 2010; Reed *et al*. 2011). For the subsequent FEA,

94   existing 3D models of *Allosaurus fragilis* and *Alligator mississippiensis* from previous

95   studies were used (Rayfield *et al*. 2001; Witmer & Ridgely 2008; Lautenschlager 2015).

96   The skull of the *Baurusuchus pachecoi* was scanned in a Toshiba Aquilion Prime

97   machine, in "Hospital das Clínicas de Ribeirão Preto", Brazil. The 1.187 slices were

98   segmented in Amira 5.3.

99   **FEA.** The 3D models of all specimens, including skulls and mandibles, were imported

100   into Hypermesh 11 (Altair Engineering) for the generation of solid tetrahedral meshes

101   (consisting of approximately 1,000,000 elements per model). For both the *Alligator* and

102   the baurusuchid models, material properties for bone and teeth were assigned based on

103   values for *Alligator mississippiensis* (bone: $E = 15.0$ GPa, $\upsilon = 0.29$, teeth: $E = 60.4$ GPa,

104   $\upsilon = 0.31$; *Porro et al*. 2011; Sellers *et al*. 2017), whereas for the *Allosaurus* model,

105   values derived from studies on theropods (bone: $E = 20.0$ GPa, $\upsilon = 0.38$, teeth: $E = 60.4$

106   GPa, $\upsilon = 0.31$; Rayfield *et al*. 2001, 2011). All material properties in the models were

107   assigned in Hypermesh and treated as isotropic and homogeneous.

108   As an intrinsic scenario for the baurusuchid, we simulated, in both the skull and

109   mandible models, a jaw adductor muscle-driven biting. The adductor muscle forces

110   were estimated using the attachment area for each muscle, based on previous works on

111   extant and extinct crocodyliforms (Holliday & Witmer 2009; Holliday *et al.* 2013). The

112   attachment area was used as a proxy for physiological cross-section area, which was

113   then multiplied by an isometric muscle stress value of 25.0 N/ cm2 (Porro *et al*. 2011).

114   To investigate the craniomandibular biomechanical properties in alternative load

115   assignments, other functional scenarios were also tested for the baurusuchid skull and

116   mandible models: unilateral bite, bilateral bite, pull-back, head-shake and head-twist.

117   The loading applied for each scenario was based on the approximation of the bite force

118   obtained from the intrinsic scenario (600 N). All loadings in the unilateral bite scenario

119   were applied to one node, perpendicular to the occlusal planes on one of the following

120   teeth: D1, D4, D9, PM2, PM3, M2 and M4. Bilateral bite scenarios were tested with the

121   same conditions as the unilateral one, but with two vectors of 300 N applied to each M4

122   and D4. The head-shake scenario was tested with two vectors of 300 N point to the

123   same direction, one on one node on the labial surface of left M2/D4 and the other on

124   one node on the lingual surface of right M2/D4. For the pull-back, the 600 N loading

125   was applied to one node at crown midheight over the distal carena of the caniniform

126   teeth (D4, PM3 and M2). For the head twist, the loadings were applied to two opposite

127   vectors of 300 N in each model. One loading vector was applied to one node at the tip

128   of the maxillary (M2) or dentary (D4) caniniform tooth, and another loading vector on

129   the opposite side on the dorsal surface of the maxilla, or ventral surface of the dentary

130   respectively.

131   Four functional scenarios were also tested in the skull and lower jaws of

132   *Allosaurus fragilis* and *Alligator mississippiensis*, for comparison. Bites were simulated

133   at comparable positions of the bites tested in the baurusuchid. Unilateral bites were

134   tested in PM2, M3, M16, D1, D4 and D13 for *Allosaurus fragilis*, and PM2, M4, M15,

135   D2, D4 and D15 for *Alligator mississippiensis*. Bilateral bites were also tested in M3

136   and D5 pairs for the theropod, and M4 and D4 pairs for the crocodylian. For meaningful

137   comparisons of form and function independent of size (Dumont et al., 2009), all models

138   were scaled to the total surface of the baurusuchid specimen.

139   For each scenario, constraints were placed on the craniomandibular articular

140   surfaces. For the skulls, three nodes were constrained on the occipital condyle, and two

141   nodes on each quadrate articular surface. For the lower jaws, three nodes on each

142   glenoid were constrained.

143

144   RESULTS

145   The bite force estimation for the baurusuchid specimen was 252 N for the skull model,

146   at the tip of the maxillary canine, and 578 N for the mandible model, at the tip of the

147   dentary canine. Considerable differences were found between the stress magnitudes of

148   the skull and lower jaws of the baurusuchid among the different scenarios tested (e.g.

149   average values of 0.4 MPa in the skull head twist and of 24.7 MPa in the bilateral biting

150   of the lower jaws). Although variable in magnitude, the stress distribution follows a

151   general pattern in the skull and lower jaws of the baurusuchid (Figure 1). The stress in

152   the skull models are mostly present in the posterior and median portions of the skull,

153   with stress hotspots located on the ventral and lateral regions of the quadrate body,

154   ventral region of the infratemporal bar, and preorbital region (anterior jugal, posterior

155   maxillae, lacrimals, nasal, prefrontals, and anterior frontal). In addition, the stress in the

156   premaxillae and maxillae are isolated from each other. This means that when loading is

157   applied to the premaxillary teeth, the maxillae remain relatively stress-free, whereas the

158   dorsal rostrum (premaxilla and nasals) is more stressed. When loading is applied to the

159   maxillary teeth, the premaxillae remain unstressed, and stress is concentrated on the

160   posterior portion of the skull (Figure1).

161   As expected, the lower jaws experienced more stress than the skull model, but

162   the stress hotspots are more homogeneously distributed, located on the dorsal surface of

163   surangular, angular and retroarticular process. Two exceptions are the jaw pull back

164   scenario, in which the stress hotspots are located around the mandibular fenestra; and

165   the bilateral bite scenario, in which most of the lower jaw is highly stressed, and only

166   the symphyseal region remain less stressed.

167   The areas around the maxillary and dentary canines remain relatively stress-free,

168   even in scenarios in which the loadings were applied to the canines. This is particularly

169   evident for the dentary canine, for which the surrounding bone remain unstressed in all

170   scenarios, including the least optimal scenario of the bilateral biting (Figure 1).

171   In general, the patterns of stress distribution we obtained for *Allosaurus* and

172   *Alligator* (which was consistent with previous studies [Rayfield *et al*. 2001; Porro *et al*.

173   2011) contrasted with that of the baurusuchid. The discrepancies are more evident on

174   the lower jaws, in which the baurusuchid remain consistently less stressed than both the

175   theropod and the crocodylian. When compared to the baurusuchid, the theropod models

176   obtained only slightly lower average stress values for the skull, but much higher values

177   for the lower jaws (Figure 2). The alligator model, in contrast, retrieved higher average

178   stress values in most scenarios than both the baurusuchid and *Allosaurus*, even though

179   the skull stress values are less discrepant (Figure 2). The only scenario that does not

180   follow this pattern is the unilateral bite at the back of the upper-tooth row, in which the

181   average stress value is similar between the baurusuchid and *Alligator*, although both

182   retrieved higher stresses than the theropod. The most discrepant results are related to the

183   mandibular anterior bite scenario, which retrieved an average stress value in *Alligator*

184   more than nine times higher than in the baurusuchid, and almost twice the average stress

185   recorded for the theropod.

186

187   DISCUSSION

188   The unexpectedly weak bite force estimated for the baurusuchid is much lower than that

189   measured for extant crocodylians of comparable size (*Alligator sinensis* with a total

190   body length around 150 cm can have a bite of up to 963N measured in caniniform

191   (Erickson *et al*. 2012). It is also only a fraction of the bite forces inferred for adult

192   theropods, which could potentially exceed 50,000 N (Gignac & Erickson 2017). This

193   weak bite force in baurusuchids suggests that their role as apex predators would

194   possibly involve hunting strategies different from most carnivorous theropods and

195   living crocodylians, which mostly rely on muscle-driven biting forces for killing

196   [Rayfield 2004, 2005, 2011; D´Amore *et al*. 2011; Erickson *et al*. 2012). As a

197   consequence, the killing potential of baurusuchids could have been enhanced by

198   structural and behavioural traits, as in other weak-bite apex predators such as

199   troodontids and allosaurid, varanid monitors and felines (Rayfield 2001; D´Amore *et al*.

200   2011; Figueirido *et al*. 2018; Torices *et al*. 2018).

201   Alternatively, the apex predator role of baurusuchids could have been a

202   historical misinterpretation, and the group would be better suited for preying on smaller

203   and/or softer animals. However, a series of craniomandibular and postcranial

204   adaptations of baurusuchids indicate otherwise. For example, the presence of extensive

205   overengineered regions around the canines in both the skull and lower jaws (e.g. regions

206   that remain relatively stress-free in all tested scenario) show that the baurusuchid

207   craniomandibular architecture could safely perform in much higher stress conditions

208   than the imposed by muscle-driving biting forces. The presence of overengineered

209   regions in *Allosaurus* has been suggested as evidence that this taxon also used

210   mechanisms to enhance killing potential in its regular feeding strategy (Rayfiled *et al*.

211   2001).

212   Additionally, the tested pull-back, head-shake and head-twist scenarios were

213 designed to understand how the baurusuchid craniomandibular architecture would

214 perform during similar head movements employed by other weak- and strong-bite apex

215 predators (Rayfield 2001; D´Amore *et al*. 2011; Torices *et al*. 2018). For baurusuchids,

216 these movements would be possible given the robust cervical vertebrae, high neural

217 spines, and well-developed cervical ribs (particularly the first two), which provided

218 large attachment areas for the muscles responsible for head lift, head twist, and side-to-

219 side movements (Cleuren & De Vree 2000; Godoy *et al*. 2018). These tests show that

220 the baurusuchid skull and mandible worked optimally in scenarios simulating non-

221 orthal loads, suggesting that baurusuchids were well suited for head movements during

222 preying, possibly even more than living crocodylians. This can be explained by the

223 combination of three skull features that minimize skull stress during bites and torsion,

224 the oreinirostral morphology, the obliterate antorbital fenestra, and extensively ossified

225 secondary palate. This combination of features is particularly efficient for stress

226 reduction during unilateral biting (Rayfield & Milner 2008).

227   Our tests also revealed that the well-developed gap between premaxillae and

228 maxillae is a unique specialization in the skull architecture of baurusuchids, very likely

229 related to predatory habits. This gap rerouted the stress from the premaxillae to the

230 dorsal surface of the fused nasals during biting, preventing stress from traveling from

231 the occlusal region of one bone to the other, and implying a functional modularity

232 between premaxillae and maxillae during bites. This gap at premaxillae-maxillae suture

233 is absent in *Allosaurus* and *Alligator*, and in those taxa, the stress travels directly from

234 the premaxilla to the maxilla, especially during the unilateral premaxillary bite

235 scenarios. A similar stress rerouting is observed in tyrannosaurids, in which the robust

236 and also fused nasals work as main route for stress distribution, bypassing the less

237   robust maxilla-lacrimal contact (Rayfield 2005). We suggest that the gap observed in

238   baurusuchids, in combination with the robust and fused nasals, worked similarly to that

239   of tyrannosaurids. The gap could also allow repeatedly punctures to be inflicted from

240   different positions of the tooth row, but concomitantly working as a built-in safety

241   factor, minimizing the risk of skull yielding (Rayfield et al., 2001). Finally, the presence

242   of ziphodont dentition in baurusuchids is also in line with the role of apex predator (Riff

243   & Kellner 2011; Godoy *et al*. 2014). The knife-like teeth with well-developed serrated

244   cutting edges is a dental adaptation for optimal defleshing of vertebrate carcasses

245   (D´Amore *et al*. 2009) and are present in a series of unrelated apex predators, including

246   theropod dinosaurs and large monitor lizards (D´Amore *et al*. 2011; Brink & Reisz

247   2014; Torices *et al*. 2018).

248   The discrepancy in the stress magnitude and distribution seen between the

249   mandibles of the three taxa suggests that this structure is also pivotal in understanding

250   the palaeoecology of baurusuchids. The stress distribution shows that *Allosaurus* and

251   *Alligator* have higher and more homogeneously distributed stress in the mandible, while

252   in the baurusuchid the stress is concentrated at the postsymphyseal region. This

253   indicates that the robust symphysis in baurusuchids is important for stabilizing the

254   lower jaws.

255   The best example of the discrepant responses among lower jaws is seen in the

256   bilateral biting scenario, for which the average stress value for the baurusuchid was

257   approximately five times greater than any other scenario. Additionally, this is the only

258   scenario in which the stress approaches the higher values presented by *Allosaurus* and

259   *Alligator* (Figure 2). The baurusuchid response is also different from *Allosaurus* and

260   *Alligator* in the sense that the average stress values in the bilateral scenarios are

261   discrepant from the unilateral bite scenarios, whereas the other two taxa show similar

262   values in both scenarios. Based on our FEA results, we propose that the bilateral biting

263   is the least likely killing strategy for baurusuchids, and the clamp-and-hold, employed

264   by living crocodylians, and large mammal predators, such as the lion (*Panthera leo*)

265   (Figueirido *et al*. 2018), does not fit the mechanical properties of baurusuchid skull.

266   Our results also indicate that baurusuchids were well adapted for handling

267   struggling preys, which were possibly subdued by inflicting a series of unilateral bites

268   using premaxillary, maxillary and particularly the dentary canines, that combined with

269   the ziphodonty would pierce repeatedly the prey skin. The puncture phase would be

270   followed by head-movements that would worsen the wounds caused by the punctures

271   and ultimately leading to the killing of the prey.

272   Our results successfully characterise the exceptional suite of biomechanical

273   properties displayed by baurusuchids, which combine exclusive adaptations, features

274   similar to theropods, and other characteristics also seen in living crocodylians. Such a

275   combination has not been reported previously for any predatory taxon, raising questions

276   on the specific evolutionary settings that allowed these features to emerge. Particularly,

277   selective pressures from extrinsic environmental factors seem to have an important

278   influence during amniote functional and biomechanical evolution (Sakamoto *et al*.

279   2019). In the case of baurusuchids, the unique Late Cretaceous palaeoecosystems of

280   southeast Brazil exhibited a combination of playa-lake systems and transitory rivers

281   which possibly permitted life to flourish in semi-arid to arid conditions (Carvalho *et al*.

282   2010; Marsola *et al*. 2016). These landmasses witnessed an extraordinary diversity of

283   crocodyliforms (especially notosuchians; Mannion *et al*. 2015), as well as other

284   tetrapods (Godoy *et al*. 2014). This resulted in a diverse array of potential preys for

285   baurusuchids, from small terrestrial crocodyliforms to gigantic titanosaur sauropods,

286   indicating that prey selection could have played an important role in the evolution of the

287   baurusuchid craniomandibular apparatus.

288

289   REFERENCES

290   Benson, R. B., Mannion, P. D., Butler, R. J., Upchurch, P., Goswami, A., & Evans, S.
291   E. (2013). Cretaceous tetrapod fossil record sampling and faunal turnover:
292   implications for biogeography and the rise of modern clades. *Palaeogeography,*
293   *Palaeoclimatology, Palaeoecology*, **372,** 88–107.

294   Bronzati, M., Montefeltro, F., & Langer, M. (2015). Diversification events and the
295   effects of mass extinctions on Crocodyliformes evolutionary history. *Royal*
296   *Society Open Science,* **2,** 140385.

297   Brink, K. S.; & Reisz, R. R. (2014). Hidden dental diversity in the oldest terrestrial apex
298   predator *Dimetrodon*. *Nature Communications*, **5,** 3269.

299   Carvalho, I., S., De Celso, A., Campos, A., & Nobre, P. (2005). *Baurusuchus*
300   *salgadoensis,* a new Crocodylomorpha from the Bauru Basin (Cretaceous),
301   Brazil. *Gondwana Research*, **8,** 11–30.

302   Carvalho, I. S., Gasparini, Z. B., Salgado, L., Vasconcellos, F. M., & Marinho, T. S.
303   (2010). Climate's role in the distribution of the Cretaceous terrestrial
304   Crocodyliformes throughout Gondwana. *Palaeogeography, Palaeoclimatology,*
305   *Palaeoecology*, **297,** 252–262.

306   Cleuren J, & De Vree, F. (2000) Feeding in Crocodilians. *In* K., Schwenk (ed.)
307   *Feeding: form, function and evolution in tetrapod vertebrates.* pp. 337–358.
308   Academic Press, San Diego.

309   D´Amore, D. C. (2009). A functional explanation for denticulation in theropod dinosaur
310   teeth. *The Anatomical Record*, **292,** 1297–1314.

311   D´Amore, D. C.; Moreno, K.; McHenry, C. R.; & Wroe, S. 2011. The effects of biting
312   and pulling on the forces generated during feeding in the Komodo dragon
313   (*Varanus komodoensis*). *PloS ONE*, **6,** e26226.

314   Dumont, E., Grosse, I., & Slater, G. (2009). Requirements for comparing the
315   performance of finite element models of biological structures. *Journal of*
316   *Theoretical Biology,* **256,** 96–103.

317   Erickson, G., Gignac, P., Steppan, S., Lappin, A., Vliet, K., Brueggen, J., Inouye, B. D.,
318   Kledzik, D., & Webb, G. (2012). Insights into the ecology and evolutionary
319   success of crocodilians revealed through bite-force and tooth-pressure
320   experimentation. *PLoS ONE,* **7,** e31781.

321 Farmer, C. G., & Sanders, K. (2010). Unidirectional airflow in the lungs of alligators.
322   *Science*, **327,** 338–340.

323 Figueirido, B.; Lautenschlager, S. Pérez-Ramos, A.; & Valkenburgh, B. (2018). Distinct
324   predatory behaviors in scimitar- and dirk-toothed sabertooth cats. *Current*
325   *Biology*, **28,** 3260–3266.

326 Gignac, P., & Erickson, G. (2017). The Biomechanics behind Extreme Osteophagy in
327   *Tyrannosaurus rex*. *Scientific Reports,* **7,** 2012.

328 Godoy, P. L. (2019). Crocodylomorph cranial shape evolution and its relationship with
329   body size and ecology. *Journal of Evolutionary Biology* (Early View).

330 Godoy, P., Benson, R., Bronzati, M., & Butler, R. (2019). The multi-peak adaptive
331   landscape of crocodylomorph body size evolution. *BMC Evolutionary Biology,*
332   **19,** 167.

333 Godoy, P., Ferreira, G., Montefeltro, F., Vila Nova, B., Butler, R., & Langer, M. (2018).
334   Evidence for heterochrony in the cranial evolution of fossil crocodyliforms.
335   *Palaeontology,* **61,** 543–558.

336 Godoy, P., Montefeltro, F., Norell, M., & Langer, M. (2014). An additional baurusuchid
337   from the cretaceous of Brazil with evidence of interspecific predation among
338   crocodyliformes. *PLoS ONE,* **9,** e97138.

339 Guillette Jr, L. J., Edwards, T. M., & Moore, B. C. (2007). Alligators, contaminants and
340   steroid hormones. *Environmental Sciences*, **14,** 331–347.

341 Holliday, C., & Witmer, L. W. (2009). The epipterygoid of crocodyliforms and its
342   significance for the evolution of the orbitotemporal region of eusuchians.
343   *Journal of Vertebrate Paleontology*, **29,** 715–733.

344 Holliday, C., Tsai, H., Skiljan, R., George, I., & Pathan, S. (2013). A 3D interactive
345   model and atlas of the jaw musculature of *Alligator mississippiensis*. *PLoS ONE,*
346   **8,** e62806.

347 Lautenschlager, S. (2015). Estimating cranial musculoskeletal constraints in theropod
348   dinosaurs. *Royal Society Open Science*, **2,** 150495

349 Lloyd, G. T., Davis, K. E., Pisani, D., Tarver, J. E., Ruta, M., Sakamoto, M., Hone, D.
350   W. E., Jennings, R., & Benton, M. J. (2008). Dinosaurs and the Cretaceous
351   terrestrial revolution. *Proceedings of the Royal Society B: Biological Sciences*,
352   **275,** 2483–2490.

353 Mannion, P., Benson, R., Carrano, M., Tennant, J., Judd, J., & Butler, R. (2015).
354   Climate constrains the evolutionary history and biodiversity of crocodylians.
355   *Nature Communications,* **6,** 8438.

356 Marsola, J. C. A., Batezelli, A., Montefeltro, F. C., Grellet-Tinner, G. & Langer, M. C.
357   (2016). Palaeoenvironmental characterization of a crocodilian nesting site from
358   the Late Cretaceous of Brazil and the evolution of crocodyliform nesting
359   strategies. *Palaeogeography, Palaeoclimatology, Palaeoecology*, **457,** 221–232.

360 Montefeltro, F. (2019). The osteoderms of baurusuchid crocodyliforms
361   (Mesoeucrocodylia, Notosuchia). *Journal of Vertebrate Paleontology*.
362   e1594242.

363 Montefeltro, F., Larsson, H., & Langer, M. (2011). A new baurusuchid
364   (Crocodyliformes, Mesoeucrocodylia) from the late cretaceous of Brazil and the
365   phylogeny of Baurusuchidae. *PLoS ONE, 6,* e21916.

366 Pol, D., & Leardi, J. (2015). Diversity patterns of Notosuchia (Crocodyliformes,
367   Mesoeucrocodylia) during the Cretaceous of Gondwana. *In* M. Fernández & Y.
368   Herrera (eds.), *Reptiles Extintos – Volumen en Homenaje a Zulma Gasparini*.
369   pp. 172–186. Buenos Aires, Argentina: Publicación Electrónica de la Asociación
370   Paleontológica Argentina.

371 Porro, L., Holliday, C., Anapol, F., Ontiveros, L., Ontiveros, L., & Ross, C. (2011).
372   Free body analysis, beam mechanics, and finite element modeling of the
373   mandible of Alligator mississippiensis. *Journal of Morphology, 272,* 910–937.

374 Rayfield, E. (2004). Cranial mechanics and feeding in *Tyrannosaurus rex. Proceedings
375   of the Royal Society B: Biological Sciences*, **271,** 1451–1459.

376 Rayfield, E. (2005). Aspects of comparative cranial mechanics in the theropod
377   dinosaurs *Coelophysis, Allosaurus* and *Tyrannosaurus. Zoological Journal of
378   the Linnean Society*, **144,** 309–316.

379 Rayfield, E. (2011). Structural performance of tetanuran theropod skulls, with emphasis
380   on the Megalosauridae, Spinosauridae and Carcharodontosauridae. *Special
381   Papers in Palaeontology*, **86,** 241–253.

382 Rayfield, E., Norman, D. B., Horner, C. C., Horner, J. R.; Smith, P. M.; Thomason, J.
383   J.; & Upchurch, P. (2001). Cranial design and function in a large theropod
384   dinosaur. *Nature*, **409,** 1033–1037.

385 Rayfield, E., & Milner, A. (2008). Establishing a framework for archosaur cranial
386   mechanics. *Paleobiology*, **34,** 494–515.

387 Reed, D. A., Porro, L. B., Iriarte-Diaz, J., Lemberg, J. B., Holliday, C. M., Anapol, F.,
388   & Ross, C. F. (2011). The impact of bone and suture material properties on
389   mandibular function in *Alligator mississippiensis*: testing theoretical phenotypes
390   with finite element analysis. *Journal of Anatomy*, **218,** 59–74.

391 Riff, D., & Kellner, A. (2011). Baurusuchid crocodyliforms as theropod mimics: Clues
392   from the skull and appendicular morphology of Stratiotosuchus maxhechti
393   (Upper Cretaceous of Brazil). *Zoological Journal of the Linnean Society,
394   **163(suppl_1**), S37–S56.

395 Sakamoto, M. (2010). Jaw biomechanics and the evolution of biting performance in
396   theropod dinosaurs. *Proceedings of the Royal Society B: Biological Sciences,
397   **277,** 3327–3333.

398   Sakamoto, M., Ruta, M., & Venditti, C. (2019). Extreme and rapid bursts of functional
399   adaptations shape bite force in amniotes. *Proceedings of the Royal Society B:*
400   *Biological Sciences*, **286,** 20181932.

401   Sellers, K., Middleton, K., Davis, J., & Holliday, C. (2017). Ontogeny of bite force in a
402   validated biomechanical model of the American alligator. *Journal of*
403   *Experimental Biology,* **220,** 2036–2046.

404   Torices, A.; Wilkinson, R.; Arbour, V. M.; Ruiz-Omenaca, J. I.; & Currie, P. J. (2018).
405   Puncture-and-pull biomechanics in the teeth of predatory coelurosaurian
406   dinosaurs. *Current Biology*, **28,** 1467–1474.

407   Wilberg, E. (2017). Investigating patterns of crocodyliform cranial disparity through the
408   Mesozoic and Cenozoic. *Zoological Journal of the Linnean Society*, **181,** 189–
409   208.

410   Witmer, L., & Ridgely, R. (2008). The paranasal air sinuses of predatory and armored
411   dinosaurs (Archosauria: Theropoda and ankylosauria) and their contribution to
412   cephalic structure. *Anatomical Record,* **291,** 1362–1388.

413   Zanno, L., & Makovicky, P. (2013). Neovenatorid theropods are apex predators in the
414   Late Cretaceous of North America. *Nature Communications,* **4,** 2827.

415

416   FIGURES AND FIGURE CAPTIONS

417

418
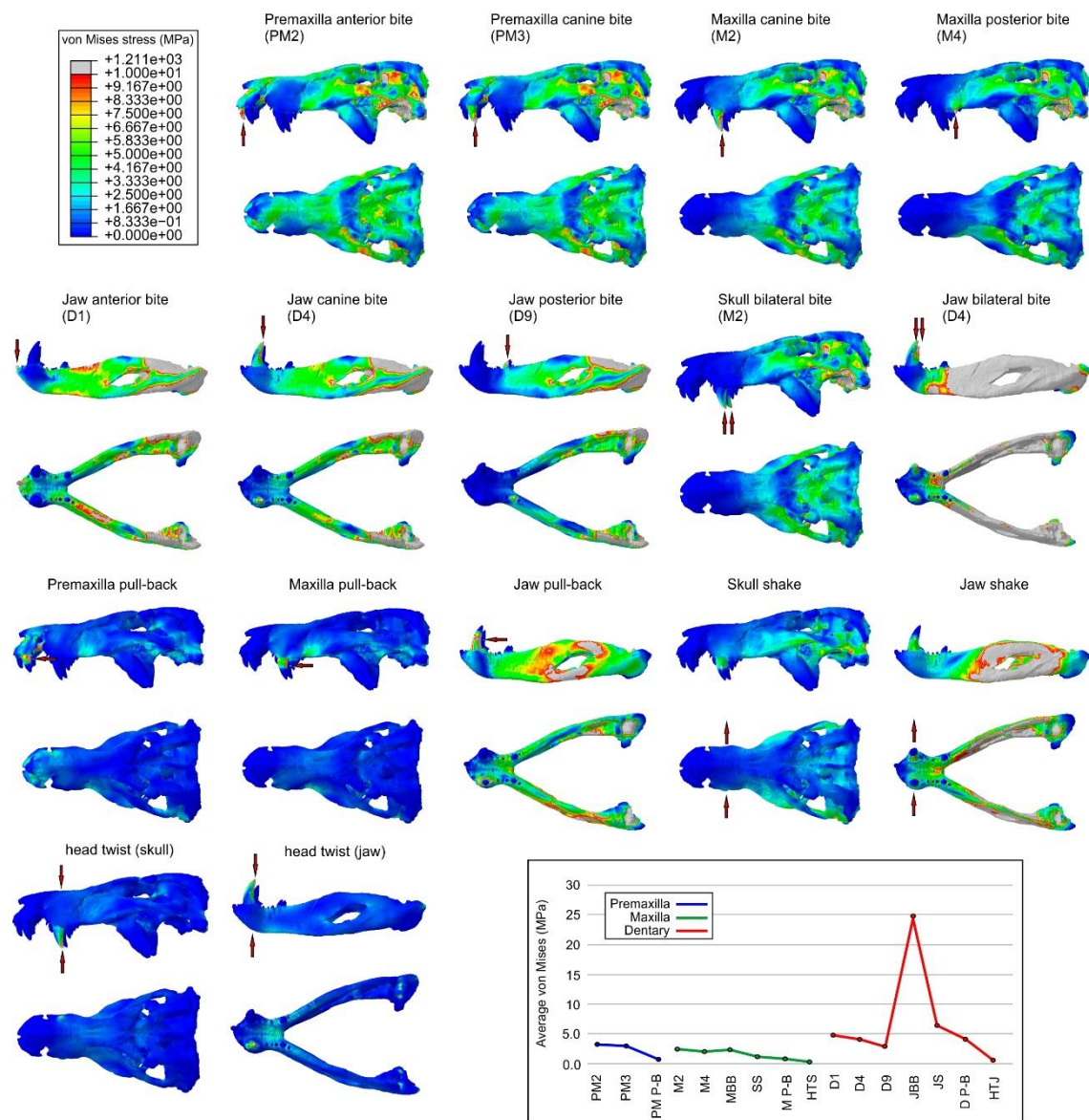
419   **Figure 1.** Von Mises stress contour plots from FEA of the baurusuchid specimen

420   LPRP/USP 0697, comparing the stress distribution of skull and mandible models under

421   distinct functional bite scenarios. Arrows indicate the location on the models of the

422   loading vectors for each scenario. Average Von Mises values per scenario are displayed

423   on the bottom right.

424

425

426
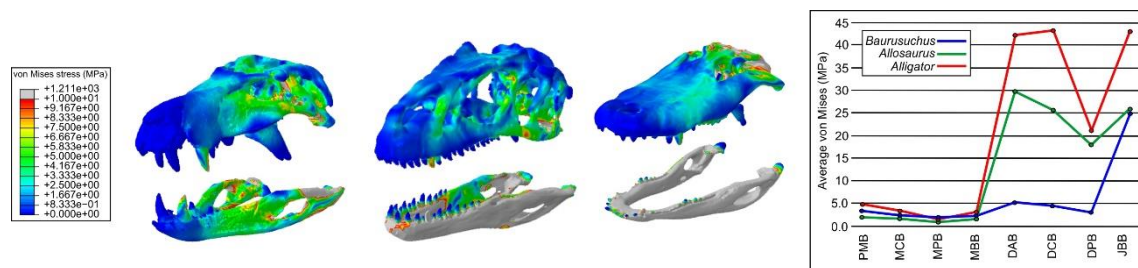
Figure 2. Comparison of Von Mises stress distribution for scaled models of different archosaurian carnivores: baurusuchid, *Allosaurus fragilis* and *Alligator mississippiensis*. Stress contour plots displayed for the anterior bite scenario. On the right, comparative average Von Mises values per scenario for each taxon.

431